locations probably participates in the lamina-specific network formation during the postnatal developmental stages.

In the developing nervous system, NO has been shown to be involved in a variety of processes concerning neural circuit formation, ranging from the refinement of axonal projections to regulating synaptic plasticity (Cramer and Sur, 1996; Gibbs and Truman, 1998; Cramer and Sur, 1999; Ernst *et al*, 1999; Wu *et al*, 2000). There is strong evidence showing that NO is involved in neural circuit formation, especially in the chick retinotectal system (Williams *et al.*, 1994; Wu *et al.*, 1994; Ernst *et al.*, 1999), the retinogeniculate projection in ferrets (Cramer *et al.*, 1996; Cramer and Sur, 1999), and the retinocollicular projection in mice (Wu *et al.*, 2000). However, Finney and Shatz (1998) elegantly demonstrated in their study using nNOS knock-out mice and specific antagonists that NO was not involved in barrel formation in the somatosensory cortex during development. A similar result was also obtained by Ruthazer *et al.* (1996). Therefore, it is reasonable to assume that the putative function of NO would be independent of the formation of cortical barrels.

Recently, McIlvain *et al.* (2003) have reported that reduced branching of thalamocortical afferent arbors in layer IV of GAP-43 (+/–) mutant cortex at P7, in which the gross formation of barrel structure at the somatosensory cortex developed normally. It is conceivable that axonal sprouting of thalamocortical afferents would be regulated independently of the barrel formation at developing somatosensory cortex. A similar finding of reduced thalamocortical sprouting at layer IV of somatosensory cortex was also demonstrated in a specific mutant strain of cortical excitatory neurons lacking *NMDA-R1* (CxNR1KO; Datwani *et al.*, 2002). Since, NMDA-R is a major upstream signal for activating nNOS in excitatory cortical neurons to produce NO (e.g. Fig. 9), the reduced thalamocortical sprouting at layer IV of CxNR1KO might stemmed from the lack of NO production at layer IV of developing somatosensory cortex. In addition, the disappearance of layer-specific NO production after the critical period of cortical plasticity (Fig. 10) seems to follow the laminar-specific shift in NMDA receptor expression on layer IV neurons, from NR2B to NR2A, at the critical period of cortical plasticity (Erisir and Harris, 2003). Taken together, we can propose a possible function of NO production in developing cortex as a promoter of thalamocortical afferent sprouting in layer IV. Such a layer-specific circuit rewiring has been reported in developing visual cortex and adult somatosensory cortex (Diamond *et al.*, 1994; Beaver *et al.*, 2001). Future studies will attempt to clarify the role of NO on the circuit formation during brain development and the importance of cortical plasticity for higher brain function.

Notes

We are very grateful to Drs Yoshinobu Sugitani and Masaharu Ogawa for technical advice. This work was supported by a Grant-in Aid for Scientific Research from the Ministry of Education, Science, Sports and Culture of Japan.

Address correspondence to Tatsuhiro Hisatsune, Department of Integrated Biosciences, The University of Tokyo, 5-1-5 Kashiwanoha, Bioscience Bldg-402, Kashiwa, Chiba 277-8562, Japan. Email: hisatsune @k.u-tokyo.ac.jp.

References

Barone P, Kennedy H (2000) Non-uniformity of neocortex: areal heterogeneity of NADPH-diaphorase reactive neurons in adult Macaque monkeys. Cereb Cortex 10:160–174.

Bayer SA, Altman J (1991) Neocortical development. New York: Raven Press.

Beaver CJ, Qinghua JI, Daw NW (2001) Layer differences in the effect of monocular vision in light- and dark-reared kittens. Vis Neurosci 18:811–820

Ben-Ari Y, Cherubini E, Corradetti R, Gaiarsa JL (1989) Giant synaptic potentials in immature rat CA3 hippocampal neurones. J Physiol 416:303–325.

Benavides-Piccione R, DeFelipe J (2003) Different populations of tyrosine-hydroxylase-immunoreactive neurons defined by differential expression of nitric oxide synthase in the human temporal cortex. Cereb Cortex 13:297–307.

Bohme GA, Bon C, Stutzmann JM, Doble A, Blanchard JC (1991) Possible involvement of nitric oxide in long-term potentiation. Eur J Pharmacol 199:379–381.

Bredt DS, Snyder SH (1989) Nitric oxide mediates glutamate-linked enhancement of cGMP levels in the cerebellum. Proc Natl Acad Sci USA 86:9030–9033.

Bredt DS, Snyder SH (1990) Isolation of nitric oxide synthetase, a calmodulin-requiring enzyme. Proc Natl Acad Sci USA 87:682–685.

Bredt DS, Snyder SH (1994) Transient nitric oxide synthase neurons in embryonic cerebral cortical plate, sensory ganglia, and olfactory epithelium. Neuron 13:301–313.

Bredt DS, Glatt CE, Hwang PM, Fotuhi M, Dawson TM, Snyder SH (1991) Nitric oxide synthase protein and mRNA are directly localized in neuronal populations of the mammalian CNS together with NADPH diaphorase. Neuron 7:615–624.

Broillet M, Randin O, Chatton J (2001) Photoactivation and calcium sensitivity of the fluorescent NO indicator 4,5-diaminofluorescein (DAF-2): implications for cellular NO imaging. FEBS Lett 491: 227–232.

Cramer KS, Sur M (1996) The role of NMDA receptors and nitric oxide in retinogeniculate development. Prog Brain Res 108:235–244.

Cramer KS, Sur M (1999) The neuronal form of nitric oxide synthase is required for pattern formation by retinal afferents in the ferret lateral geniculate nucleus. Brain Res Dev Brain Res 116:79–86.

Cramer KS, Angelucci A, Hahm JO, Bogdanov MB, Sur M (1996) A role for nitric oxide in the development of the ferret retinogeniculate projection. J Neurosci 16:7995–8004.

Datwani A, Iwasato T, Itohara S, Erzurumlu RS (2002) NMDA receptor-dependent pattern transfer from afferents to postsynaptic cells and dendritic differentiation in the barrel cortex. Mol Cell Neurosci 21:477–492.

Dawson TM, Bredt DS, Fotuhi M, Hwang PM, Snyder SH (1991) Nitric oxide synthase and NADPH diaphorase are identical in brain and peripheral tissues. Proc Natl Acad Sci U S A 88:7797–7801

Derer P, Derer M (1993) Ontogenesis of NADPH-diaphorase neurons in the mouse forebrain. Neurosci Lett 152:21–24

Diamond ME, Wei Huang, Ebner FF (1994) Laminar comparison of somatosensory cortical plasticity. Science 265:1885–1888

Erisir A, Harris JL (2003) Decline of the critical period of visual plasticity is concurrent with the reduction of NR2B subunit of the synaptic NMDA receptor in layer 4. J Neurosci 23:5208–5218

Ernst AF, Wu HH, El-Fakahany EE, McLoon SC (1999) NMDA receptor-mediated refinement of a transient retinotectal projection during development requires nitric oxide. J Neurosci 19:229–235.

Finney EM, Shatz CJ (1998) Establishment of patterned thalamocortical connections does not require nitric oxide synthase. J Neurosci 18:8826–8838.

Fukuda S, Kato F, Tozuka Y, Yamaguchi M, Miyamoto Y, Hisatsune T (2003) Two distinct subpopulations of nestin-positive cells in adult mouse dentate gyrus. J Neurosci 23:9357–9366.

Garthwaite J, Charles SL, Chess-Williams R (1988) Endothelium-derived relaxing factor release on activation of NMDA receptors suggests role as intercellular messenger in the brain. Nature 336:385–388.

Gibbs SM, Truman JW (1998) Nitric oxide and cyclic GMP regulate retinal patterning in the optic lobe of *Drosophila*. Neuron 20:83–93.

Higashi S, Crair MC, Kurotani T, Inokawa H, Toyama K (1999) Altered spatial patterns of functional thalamocortical connections in the barrel cortex after neonatal infraorbital nerve cut revealed by optical imaging. Neuroscience 91:439–452.

Higashi S, Molnar Z, Kurotani T, Toyama K (2002) Prenatal development of neural excitation in rat thalamocortical projections studied by optical imaging. Neuroscience 115:1231-1246.

Iwasato T, Datwani A, Wolf AM, Nishiyama H, Taguchi Y, Tonegawa S, Knopfel T, Erzurumlu RS, Itohara S (2000) Cortex-restricted disruption of NMDAR1 impairs neuronal patterns in the barrel cortex. Nature 406:726-731.

Jacobowitz DM, Abbott LC (1998) Developing mouse brain. Boca Raton, FL: CRC Press.

Knowles RG, Palacios M, Palmer RM, Moncada S (1989) Formation of nitric oxide from L-arginine in the central nervous system: a transduction mechanism for stimulation of the soluble guanylate cyclase. Proc Natl Acad Sci U S A 86:5159-5162.

Kojima H, Nakatsubo N, Kikuchi K, Kawahara S, Kirino Y, Nagoshi H, Hirata Y, Nagano T (1998a) Detection and imaging of nitric oxide with novel fluorescent indicators: diaminofluoresceins. Anal Chem 70:2446-2453.

Kojima H, Nakatsubo N, Kikuchi K, Urano Y, Higuchi T, Tanaka J, Kudo Y, Nagano T (1998b) Direct evidence of NO production in rat hippocampus and cortex using a new fluorescent indicator: DAF-2 DA. Neuroreport 9:3345-3348.

Kojima H, Hirotani M, Nakatsubo N, Kikuchi K, Urano Y, Higuchi T, Hirata Y, Nagano T (2001) Bioimaging of nitric oxide with fluorescent indicators based on the rhodamine chromophore. Anal Chem 73:1967-1973.

Leamey CA, Ho-Pao CL, Sur M (2003) Role of calcineurin in activity-dependent pattern formation in the dorsal lateral geniculate nucleus of the Ferret. J Neurobiol 56:153-162.

Lopez-Bendito G, Molnar Z (2003) Thalamocortical development: how are we going to get there? Nat Rev Neurosci 4:276-289.

McIlvain VA, Robertson DR, Maimone MM, McCasland JS (2003) Abnormal thalamocortical pathfinding and terminal arbors lead to enlarged barrels in neonatal GAP-43 heterozygous mice. J Comp Neurol 462:252-264.

Mitrovic N, Schachner M (1996) Transient expression of NADPH diaphorase acitivity in the mouse whisker to barrel field pathway. J Neurocytol 25:429-437.

Miyakawa N, Uchino S, Yamashita T, Okada H, Nakamura T, Kaminogawa S, Miyamoto Y, Hisatsune T (2002) A glycine receptor antagonist, strychnine, blocked NMDA receptor activation in the neonatal mouse neocortex. Neuroreport 13:1667-1673.

Molnar Z, Higashi S, Adams R, Toyama K (2000) Earliest interactions between thalamus and cortex. In: Plasticity of adult barrel cortex (Kossut M, ed.), pp. 47-80. Johnson City, TN: FP Graham.

Okada H, Miyakawa N, Mori H, Mishina M, Miyamoto Y, Hisatsune T (2003) NMDA receptors in cortical development are essential for the generation of coordinated increases in $[Ca^{2+}]_i$ in 'neuronal domains'. Cereb Cortex 13:749-757.

Owens DF, Boyce LH, Davis MB, Kriegstein AR (1996) Excitatory GABA responses in embryonic and neonatal cortical slices demonstrated by gramicidin perforated-patch recordings and calcium imaging. J Neurosci 16:6414-6423.

Rivier F, Clarke S (1997) Cytochrome oxidase, acetylcholinesterase, and NADPH-diaphorase staining in human supretemporal and insular cortex: evidence for multiple auditory areas. Neuroimage 6:288-304.

Ruthazer ES, Gillespei DC, Dawson TM, Snyder SH, Stryker MP (1996) Inhibition of nitric oxide synthase does not prevent ocular dominance plasticity in kitten visual cortex. J Physiol (Lond) 494:519-527.

Santacana M, Uttenthal LO, Bentura ML, Fernandez AP, Serrano J, Martinez de Velasco J, Alonso D, Martinez-Murillo R, Rodrigo J (1998) Expression of neuronal nitric oxide synthase during embryonic development of the rat cerebral cortex. Brain Res Dev Brain Res 111:205-222.

Schambra UB, Lauder JM, Silver J (1992) Prenatal mouse brain. San Diego: Academic Press.

Sharp CD, Hines I, Houghton J, Warren A, Jackson TH 4th, Jawahar A, Nanda A, Elrod JW, Long A, Chi A, Minagar A, Alexander JS (2003) Glutamate causes a loss in human cerebral endothelial barrier integrity through activation of NMDA receptor. Am J Physiol Heart Circ Physiol. 285:2592-2598.

Sugitani Y, Nakai S, Minowa O, Nishi M, Jishage K, Kawano H, Mori K, Ogawa M, Noda T (2002) Brn-1 and Brn-2 share crucial roles in the production and positioning of mouse neocortical neurons. Genes Dev 16:1760-1765.

Sur M, Leamey CA (2001) Development and plasticity of cortical areas and networks. Nat Rev Neurosci 2:251-262.

Terada H, Nagai T, Okada S, Kimura H, Kitahama K (2001) Ontogenesis of neurons immunoreactive for nitric oxide synthase in rat forebrain and midbrain. Brain Res Dev Brain Res 128:121-137.

Van Eden CG, Steinbusch HWM, Rinkens A, de Vente J (1996) Developmental patten of NADPH-diaphorase activity and nitric oxide-stimulated cGMP immunoreactivity in the frontal rat cortex and its role in functional recovery from aspiration lesions. J Chem Neuoroanat 10:279-286.

Vercelli A, Repici M, Biasiol S, Jhaveri S (1999) Maturation of NADPH-d activity in the rat's barrel-field cortex and its relationship to cytochrome oxidase activity. Exp Neurol 156:294-315.

Welker C, Woolsey TA (1974) Structure of layer IV in the somatosensory neocortex of the rat: description and comparison with the mouse. J Comp Neurol. 158:437-453

Wiencken AE, Casagrande VA (2000) The distribution of NADPH diaphorase and nitric oxide synthetase (NOS) in relation to the functional compartments of areas V1 and V2 of primate visual cortex. Cereb Cortex 10:499-511.

Williams CV, Nordquist D, McLoon SC (1994) Correlation of nitric oxide synthase expression with changing patterns of axonal projections in the developing visual system. J Neurosci 14:1746-1755.

Wong-Riley M, Anderson B, Liebl W, Huang Z (1998) Neurochemical organization of the macaque striate cortex: correlation of cytochrome oxidase with Na+K+ATPase, NADPH-diaphorase, nitric oxide synthase, and *N*-methyl-D-aspartate receptor subunit 1. Neuroscience 83:1025-1045.

Wu HH, Williams CV, McLoon SC (1994) Involvement of nitric oxide in the elimination of a transient retinotectal projection in development. Science 265:1593-1596.

Wu HH, Cork RJ, Huang PL, Shuman DL, Mize RR (2000) Refinement of the ipsilateral retinocollicular projection is disrupted in double endothelial and neuronal nitric oxide synthase gene knockout mice. Brain Res Dev Brain Res 120:105-111.

Yan XX, Garey LJ, Jen LS (1996) Prenatal development of NADPH-diaphorase-reactive neurons in human frontal cortex. Cereb Cortex 6:737-745.

Tissue Antigens ISSN 0001-2815

Identification and analysis of MHC class II DRB1 (Patr-DRB1) alleles in chimpanzees

E. J. Bak[1], Y. Ishii[1], T. Omatsu[1], S. Kyuwa[1], T. Tetsuya[2], I. Hayasaka[2] & Y. Yoshikawa[1]

1 Department of Biomedical Science, Graduate School of Agricultural and Life Sciences,The University of Tokyo, Tokyo 113-8657, Japan
2 Kumamoto Primate Research Park, Sanwa Kagaku Kenkyusho. Co., Ltd, 990 Misumimachiootao, Uki, 869-3201, Japan

Key words
allelic polymorphism; microsatellite repeat length variability; Patr-DRB1 allele; PCR technique

Correspondence
Eun Jung Bak
Department of Biomedical Science
Graduate School of Agricultural and Life Sciences
The University of Tokyo
1-1-1 Yayoi
Bunkyo-ku
Tokyo 113-8657
Japan
Tel: 81 3 5841 5038
Fax: 81 3 5841 8186
e-mail: missbakej@yahoo.co.jp

Received 19 August 2005; revised 5 October 2005; accepted 7 November 2005

doi: 10.1111/j.1399-0039.2005.00539.x

Abstract

The *MHC-DRB1* gene is known to display the most extensive allelic polymorphisms among MHC class II genes. We attempted the selective identification of chimpanzee (*Pan troglodytes*) DRB1 (Patr-DRB1) alleles using the polymerase chain reaction (PCR) technique in three steps: first, we performed Patr-DRB1*02 lineage-specific 8-kb PCR for *02 lineage detection in each chimpanzee; second, we performed 620-bp PCR for amplification of full-length exon 2; and finally, we carried out an insert check using the pattern of microsatellite repeat length variability. In the genomic DNA of 23 chimpanzees, nine Patr-DRB1 alleles containing two new alleles were detected. Our approach provides a relatively effective method of identifying Patr-DRB1 alleles in individual chimpanzees and should also contribute to our understanding of the features of MHC molecules in non-human primates.

Introduction

The classical major histocompatibility complex (MHC) class II molecules are heterodimeric surface glycoproteins composed of polymorphic α and β chains (1–3). MHC class II molecules play a key role in orientation in the immune response due to their restricted expression on professional antigen-presenting cells (APCs) (4, 5). Additionally, differential peptide binding of distinct MHC class II molecules can lead to different T-helper cell activation, and MHC class II molecules are therefore associated with susceptibility or resistance to infectious diseases (6, 7).

Chimpanzees have a significantly favorable response to human immunodeficiency virus (HIV)-1 and human hepatitis B virus (HBV) (8, 9). Furthermore, the chimpanzee model of human hepatitis C virus (HCV) infection is suitable for determining the identity of epitopes targeted by $CD4^+$ cells.

High levels of genetic homology between chimpanzees (*Pan troglodytes*) and humans are a major reason why the chimpanzee represents an important experimental animal for comparative bioscience (10). In both humans and chimpanzees, the MHC class II genes are divided into DP, DQ, and DR subregions. The DR subregion appears to display the most extensive polymorphism in MHC class II genes in which the β chain is encoded by any of a series of polymorphic DRB loci, while the α chain is encoded by the virtually monomorphic DRA locus (11, 12). Chimpanzees have three functional loci (DRB1, DRB3, and DRB5) among several DRB loci (DRB1, DRB3, DRB4, DRB5, DRB6, DRB7, DRW8, and DRW9). The functional DRB loci are characterized by an extensive amount of allelic variation that is confined primarily to the second exon. Patr-DRB2, Patr-DRB8, and Patr-DRB9, denoted as HLA-DRB2, HLA-DRB8, and HLA-DRB9, respectively, are thought to be present, but the alleles have not yet been determined (13).

The analysis of the *DRB1* gene among the DR regions has generally been considered to be the most important

parameter for studying phylogeny and disease association (14–18). In particular, the *Patr-DRB1* gene has been shown to be the most polymorphic of the functional *DRB* genes (2). Therefore, a rapid and precise typing method for *DRB1* genes is necessary for defining polymorphisms and performing sequence analysis of a large number of individuals for group management as well as for genetic analysis of disease susceptibility. In the present study, we developed a useful method for the determination of Patr-DRB1 alleles and examined Patr-DRB1 allelic diversity in a chimpanzee group in Japan.

Materials and methods

DNA samples

The 23 chimpanzees used in this study were housed at the Kumamoto Primate Park, Sanwa Kagaku Kenkyusho, in Japan. The name, registration number, age, and sex of each animal are listed in Table 1. All but six of the chimpanzees (Miyuki, Kirara, Kurara, Kotetu, Paru, and Zugo) were captured in Africa and transported to Japan. The genetic relationships among the chimpanzees are summarized in Figure 1. To the best of our knowledge, there were no other genetic relationships among the chimpanzees used in this study. The pedigree of this chimpanzee colony is provided at http://www.nbr-chimp.org/chim/zoo/sanwa/sanwa-m_all.html.

Table 1 Patterns of Patr-DRB1 alleles in individual chimpanzee

Name	No.	Age	Sex	Patr-DRB1
Ichigo	115	25	♀	*0302, *0307
Iyo	C54	28	♀	*0204, *0307
Izou	24	27	♂	*0201, *0311
Kirara	277	9	♀	*0305, *0307
Koiko	C51	28	♀	*0307
Konatu	105	28	♀	*0312
Kotetu	244	15	♂	*0201, *0312
Kurara	278	9	♀	*0305, *0307
Maruku	109	25	♂	*0204, *0302
Miyuki	204	20	♀	*0204, *0305
Nozomi	112	27	♀	*0302
Paru	228	16	♀	*0307
Remu	106	24	♀	*0201, *0204
Roman	C69	31	♀	*0201, *0307
Sango	C35	29	♀	*0204, *0307
Sanzou	C33	31	♂	*0201, *0307
Siomi	85	25	♀	*1001, *0302
Sumiko	86	25	♀	*0309
Susumu	82	27	♂	*0307
Takabo	104	28	♂	*0201, *0311
Tamae	108	26	♀	*0204, *0302
Tetu	45	29	♂	*0204, *0307
Zugo	256	13	♂	*0307

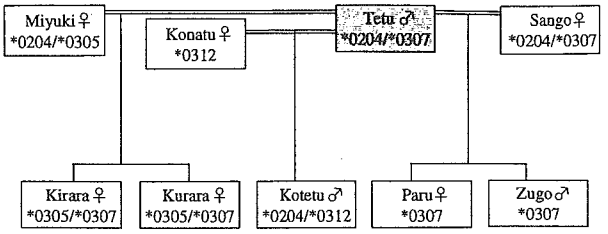

Figure 1 Pedigree patterns of the three chimpanzee families. The horizontal and vertical bars mean the partner (double line) and thier progenies (single line), respectively. Tetu (gray box) is an alpha male.

Genomic DNA was isolated from a peripheral blood sample using a QIAamp DNA Blood Mini Kit according to the manufacturer's instructions (Qiagen, Hilden, Germany).

Design of the primer set for Patr-DRB1 exon 2

In order to determine a specific primer pair which amplifies exon 2 in each Patr-DRB1 allele, 8-kb polymerase chain reaction (PCR) covering the area from exon 1 to exon 3 on the *DRB1* gene was performed using the genomic DNA of Sanzou and Iyo (Figure 2A,B). The primer pair (DRB-E1+ and DRB-E3–) was designed from a Patr-DR cDNA clone as previously described (19). The reaction mixture contained 0.25 U of LA Taq polymerase (Takara, Kyoto, Japan), 2.5 mM dNTP, 2.5 mM $MgCl_2$, 4 μM of each primer, and 2 μl of DNA template. Amplification was first performed for 14 cycles of denaturation at 94°C for 20 s with annealing and extension at 68°C for 20 min. This process was followed by 17 cycles of denaturation at 94°C for 20 s with annealing and extension at 68°C for 20 min in a stepwise elongation with an incubation time of 15 s/cycle. Only one band of 8 kb was detected during electrophoresis with an 0.8% agarose gel (Wako, Osaka, Japan). The purified 8-kb target product was ligated into a pCR-XL-TOPO vector (Invitrogen, Carlsbad, CA) and then transformed into a DH5™ competent cell (Toyobo, Osaka, Japan). The obtained clones were checked by PCR with the primer pair (sense: 5′-GCTTCGACAGCGACGTGGGGGAGT-3′; antisense: 5′-ACCCGCTCCGTCCCATTGAAGAAA-3′) that was used to amplify the 250-bp product of the chimpanzee DRB1 exon 2. Each of three plasmid clones from Sanzou and Iyo was isolated with a Nucleospin® Plasmid QuickPure kit (Macherey-Nagel, Düren, Germany).

The plasmid samples were labeled with a Big Dye™ Terminator v3.1 Cycle Sequencing Kit (Applied Biosystems, Foster City, CA) and analyzed with an ABI PRISM™ 377 DNA Sequencer (Applied Biosystems). Based on the sequence, the PCR primer pair for each chimpanzee was designed (DRB-Int1+ and

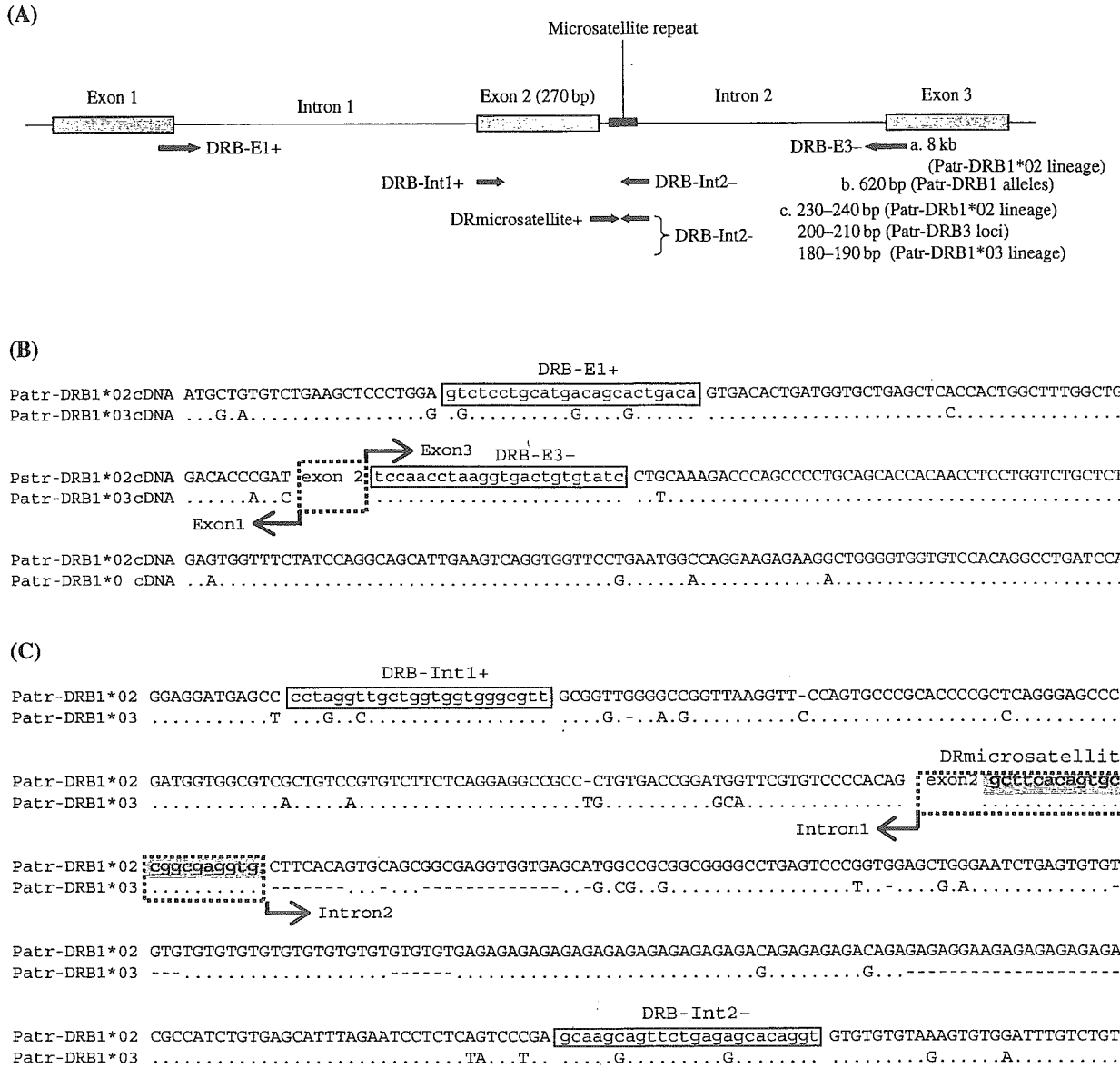

Figure 2 (A) Schematic diagram of the primer pairs used in this study. (a) 8-kb PCR for the detection of Patr-DRB1*02 lineage. (b) 620-bp PCR for the exon 2 amplification of Patr-DRB1 alleles. (c) An insert check for colony selection of Patr-DRB1 alleles. (B) A primer pair for 8-kb PCR. DRB-E1+ and DRB-E3– (a white rectangle) are located in exons 1 and 3, respectively. The upper and lower nucleotide sequences are the Patr-DRB1*02 lineage cDNA and Patr-DRB1*03 lineage cDNA (accession number AY663401), respectively. Dots (.) indicate identity with the Patr-DRB1*02 lineage. Exon 2 sequences are omitted. (C) Primer pairs for the exon 2 fragments and insert checking. The upper and lower nucleotide sequences are the Patr-DRB1*02 lineage and Patr-DRB1*03 lineage, respectively. Dots (.) indicate identity with the Patr-DRB1*02 lineage. Dashes (–) indicate the deleted sequence. The primer pairs for exon 2 appear inside the white rectangular boxes (DRB-Int1+ and DRB-Int2–). The primer pair for the insert check in clones appears in the gray and white boxes (DRmicrosatellite+ and DRB-Int2–). PCR, polymerase chain reaction.

DRB-Int2–; Figure 2A,C) to amplify a 620-bp product containing the entire exon 2 (270 bp) sequences. In addition, amplification of Patr-DRB1 lineages other than the Patr-DRB1*02 lineage was confirmed in one other chimpanzee (Siomi).

PCR, cloning, and the selection of DRB1 clones

PCR was applied to the DNA of the 23 chimpanzees as follows. Amplification was performed using AmpliTaq Gold (Applied Biosystems) with DRB-Int1+ and DRB-

Int2– primers, and the 620-bp products were cloned into a pCRII-TOPO vector (Invitrogen). Due to the high genetic homology of *Patr-DRB1*03* and the *DRB3* gene, the target products were detected in both the *DRB1* and *DRB3* genes (sequence data of detected Patr-DRB3 not shown). In order to select only DRB1 alleles, a specific insert check was carried out on the 12 selected clones. A new sense primer (DRmicrosatellite+) was designed from the microsatellite repeat region of intron 2, and PCR was carried out (Figure 2A,C). Identification of amplified products was performed on the 8% acrylamide gel. Based on the results of the electrophoresis, we again selected 6–8 clones of DRB1 alleles and sequenced them.

MHC Patr-DRB1 nomenclature

The official designation for the Patr-DRB1 allele detected in the present study was obtained from IMGT-NHP database (20). New alleles have been registered in the DNA Data Bank of Japan (DDBJ).

Results

Specific separation of DRB1 alleles in individual chimpanzees and microsatellite repeat patterns of each allele

In the DRB1 loci of the HLA, the lengths from exon 1 to exon 3 containing intron 1 on the HLA-DRB1*15 and HLA-DRB1*16 lineages (denoted as the Patr-DRB1*02 lineage in chimpanzees) and the HLA-DRB1*03 lineage (denoted as the Patr-DRB1*03 lineage in chimpanzees) (21) were approximately 8 and 11 kb, respectively. Similarly, the lengths from exon 1 to exon 3 of the Patr-DRB1*03 lineage was approximately 11 kb (accession number, AY663401).

In the present study, we were able to identify the existence of a Patr-DRB1*02 lineage by the amplification of 8 kb using the DRB-E1+ and DRB-E3– primer pair [Figure 2A, (a)]. Nine (Kirara, Kurara, Ichigo, Nozomi, Koiko, Susumu, Sumiko, Paru, and Zyugo) of the 23 chimpanzees did not have the target band of 8 kb. In fact, the Patr-DRB1*02 lineage was not detected in these chimpanzees in their sequence analysis (Table 1). We next amplified the second exon of DRB1 alleles with a 620-bp primer pair [Figure 2A, (b)] and cloned it in vector. We then attempted to carry out an insert check with the new primer pair [DRmicrosatellite+ and DRB-Int2–; Figure 2A, (c)]. Sequence analysis indicated that the lengths of the allele-specific PCR product were the following: the Patr-DRB1*02 lineage, Patr-DRB3 locus, and Patr-DRB1*03 lineage were 230–240, 200–210, and 180–190 bp, respectively (Figure 3). As a consequence, the detection quality of the DRB1 alleles was maximized

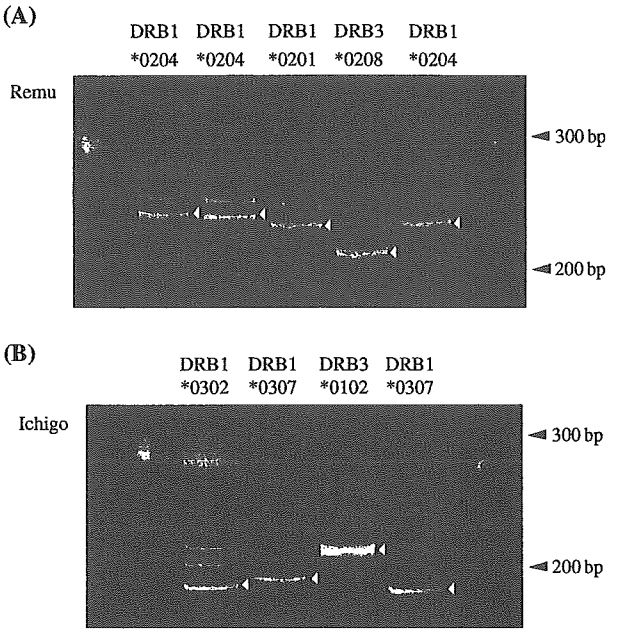

Figure 3 An acrylamide gel for each of the clones derived from Remu and Ichigo. PCR products were amplified by a DRmicrosatellite+ and DRB1-Int2– primer. The target band for each clone is represented by a white triangle. (A) Remu shows DRB1*0201, DRB1*0204, and DRB3*0208. (B) Ichigo shows DRB1*0302, DRB1*0307, and DRB3*0102. PCR, polymerase chain reaction.

by the present PCR technique and we were able to effectively detect the DRB1 alleles in each chimpanzee.

Moreover, we analyzed allelic diversity using a complex microsatellite located in intron 2, close to the polymorphic second exon. The detected polymorphism in the intron 2 microsatellite displays a complex pattern, with both sequence and length variability between alleles (Table 2).

Patterns of Patr-DRB1 alleles in individual chimpanzees

The patterns of the Patr-DPB1 alleles in each chimpanzee are summarized in Table 1. Nine alleles, including two new alleles (Patr-DRB1*0311 and Patr-DRB1*0312), were detected in this study and could be divided into three lineages: the Patr-DRB1*02 lineage, which included the Patr-DRB1*0201 and Patr-DRB1*0204 alleles; the Patr-DRB1*03 lineage, which included the Patr-DRB1*0302, Patr-DRB1*0305, Patr-DRB1*0307, Patr-DRB1*0309, Patr-DRB1*0311, and Patr-DRB1*0312 alleles; and the Patr-DRB1*10 lineage, which included only the Patr-DRB1*1001 allele. In this study, the Patr-DRB1*07 lineage was not detected.

The majority of chimpanzees (16/23) showed heterozygotes that combined with the DRB1*02 (1/16), DRB1*02/03 (11/16), DRB1*03/03 (3/16), and DRB1*1001 allele/03 lineages (1/16). The Patr-DRB1*0307 allele was found in

Table 2 Microsatellite variation of alleles detected in this study

Allele	5′ repeat	Middle repeat	3′ repeat	Dinucleotide$^-$ repeat number of a complex microsatellite
Patr-DRB1*0201	$(GT)_{19-20}$	$(GA)_{11-12}CA(GA)_4CA(GA)_3GGAA$	$(GA)_6$	47–49
Patr-DRB1*0204	$(GT)_{16}$	$(GA)_{14}CA(GA)_4CA(GA)_3GGAA$	$(GA)_6$	47
Patr-DRB1*0302	$(GT)_{21}$	$(GA)_6AA$	$(GA)_6$	34
Patr-DRB1*0305	$(GT)_{16}$	$(GA)_4AA$	$(GA)_7$	28
Patr-DRB1*0307	$(GT)_{11}$	. . .	$(GA)_{21}$	32
Patr-DRB1*0309	$(GT)_{10}$	$(GA)_{18}CA$	$(GA)_4$	33
Patr-DRB1*0311	$(GT)_{20}$	$(GA)_5AA$	$(GA)_6$	32
Patr-DRB1*0312	$(GT)_9$	$(GA)_{16}CA$	$(GA)_4$	30
Patr-DRB1*1001	$(GT)_9$	$(GA)_{11}CA(GA)_4AA$	$(GA)_4$	30
Patr-DRB3*0208	$(GT)_6$	$(GA)_{14}(GA)_9GGAA(GA)_4CA$	$(GA)_3$	39
Patr-DRB3*0102	$(GT)_2$	$(GT)_7AT(GT)_6(GA)AA(GA)_6GGAA(GA)_4CA$	$(GA)_3$	38

13 chimpanzees. The identical twin chimpanzees, Kirara and Kurara, were found to share Patr-DRB1*0307 (Figure 1).

Sequence analysis of the Patr-DRB1 allele

The nucleotide sequences of Patr-DRB1 exon 2 and the deduced amino acid sequences are depicted in Figures 4 and 5, respectively. None of the alleles, including the two new alleles, displayed features characteristic of a pseudogene.

The common sequence motifs were concentrated in the upstream region in the exon 2 segment (codon 9–45) within the Patr-DRB1 lineages. All of the Patr-DRB1*03 lineages containing the two new alleles were found to show the EYSTS amino acid motif at positions 9–13 (the gray rectangular box in Figure 5). In addition, the Patr-DRB1*02 lineage was found to share an identical EEFMRFDSDV amino acid motif at positions 35–44 and the LQPKG amino acid motif at positions 9–13 (except the Patr-DRB1*0205 allele; solid-lined boxes in Figure 5). The FLDRYFY motif at positions 26–32 was found in two Patr-DRB1*02 alleles (Patr-DRB1*0202 and Patr-DRB1*0205) and six Patr-DRB1*03 alleles (Patr-DRB1*0306, Patr-DRB1*0308, Patr-DRB1*0309, Patr-DRB1*0310, Patr-DRB1*0311, and Patr-DRB1*0312; dotted-lined box in Figure 5).

On the other hand, there appeared to be broad variation in the downstream region of exon 2 (codon 60–90). The variations of the two new alleles (Patr-DRB1*0311 and Patr-DRB1*0312) were found in this region. Patr-DRB1*0311 was similar to Patr-DRB1*0310, but a different non-synonymous substitution was found at codon 84 (Gly→Arg; the gray box in Figure 4). Additionally, Patr-DRB1*0312 was similar to Patr-DRB1*0309, but two non-synonymous substitutions were found at codon 57 (Asp→Ser) and codon 61 (Trp→Tyr; solid-lined box in Figure 4). Furthermore, several alleles were encoded to valine, alanine, and leucine at position 86; Patr-DRB1*0305, Patr-DRB1*0306, and Patr-DRB1*0310 were changed to valine, Patr-DRB1*0307, Patr-DRB1*0309, and Patr-DRB1*0312 to alanine, and Patr-DRB1*0701 to leucine.

Discussion

Studies of the MHC class II DR molecule have been progressing with the intent of developing therapeutic and preventive vaccines (22). Specifically, the influence of $CD4^+$ T cells against individual epitopes in HCV has been studied in humans and chimpanzees (10, 23). Most individual epitopes fit the DR supertype motif and show high affinities with the DRB1 molecule, DRB1*1001, DRB1*0701, and DRB1*0402. It is believed that DRB1 alleles may play an important role in vaccine development.

Useful identification of MHC DRB alleles in the rhesus macaque (*Macaca mulatta*) and common marmoset (*Callithrix jacchus*) has been achieved through denaturing gradient gel electrophoresis (DGGE) and PCR-single-strand conformation polymorphism (PCR-SSCP) (24–26). In the chimpanzee, the traditional approach for typing DRB alleles involves cloning and sequencing methods using PCR (1, 2, 10, 21). However, DNA sequencing specific to each *DRB* gene from individual chimpanzees has been difficult, because there is high genetic homology within functional DRB loci. The traditional approach for cloning and sequencing exon 2 on *DRB* genes for a given colony has been reported to be disadvantageous, in which a minimum of 30 different molecular clones must be selected (10). Furthermore, in our preliminary experiments using the primer set derived in a previous study (1), we were unable to detect DRB1 alleles among 25–30 different clones in the tested chimpanzees (data not shown). Therefore, in the present study, we hypothesized that a PCR technique using three separate steps could facilitate the identification and characterization of unique Patr-DRB1 alleles and provide a rapid and unambiguous detection method for Patr-DRB1 alleles.

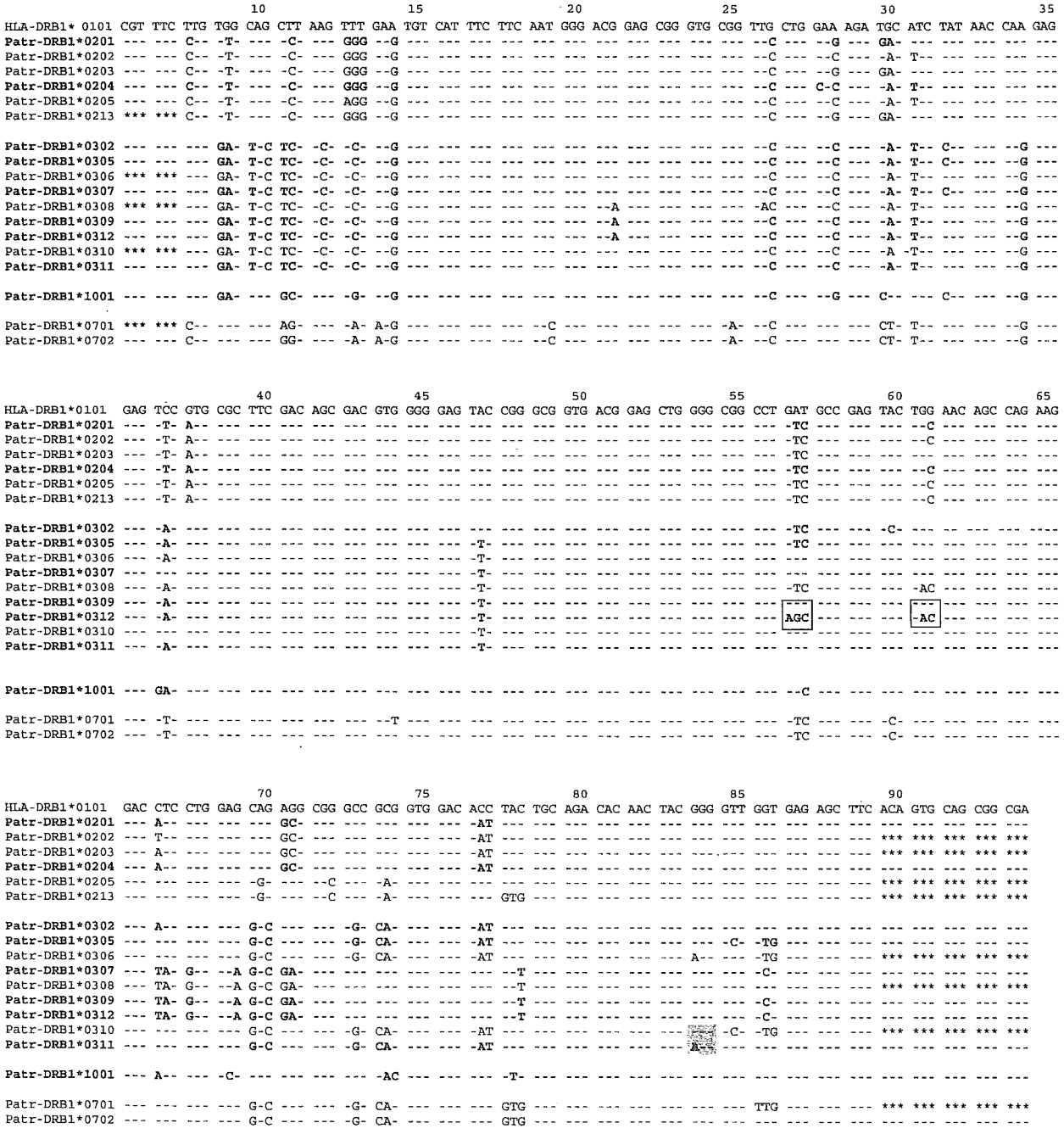

Figure 4 Alignment of the nucleotide sequences of Patr-DRB1 exon 2 alleles. The seven known alleles and two new alleles detected in this study are highlighted by bold print (Patr-DRB1*0311, DDBJ accession number AB201752; Patr-DRB1*0312, DDBJ accession number AB201753). An HLA-DRB1*0101 allele is given at the top. Dashes (–) indicate identity with the consensus sequence and the asterisk (*), a lack of availability of sequence information.

We were able to analyze the full length of exon 2 on Patr-DRB1 loci using a 620-bp primer pair. The sequence data of exon 2 of Patr-DRB1 alleles suggest that the β-pleated sheet and the α-helical portion have evolved distinctly from one another. In the β-pleated sheet portions, similar amino acid motifs within the Patr-DRB1*02

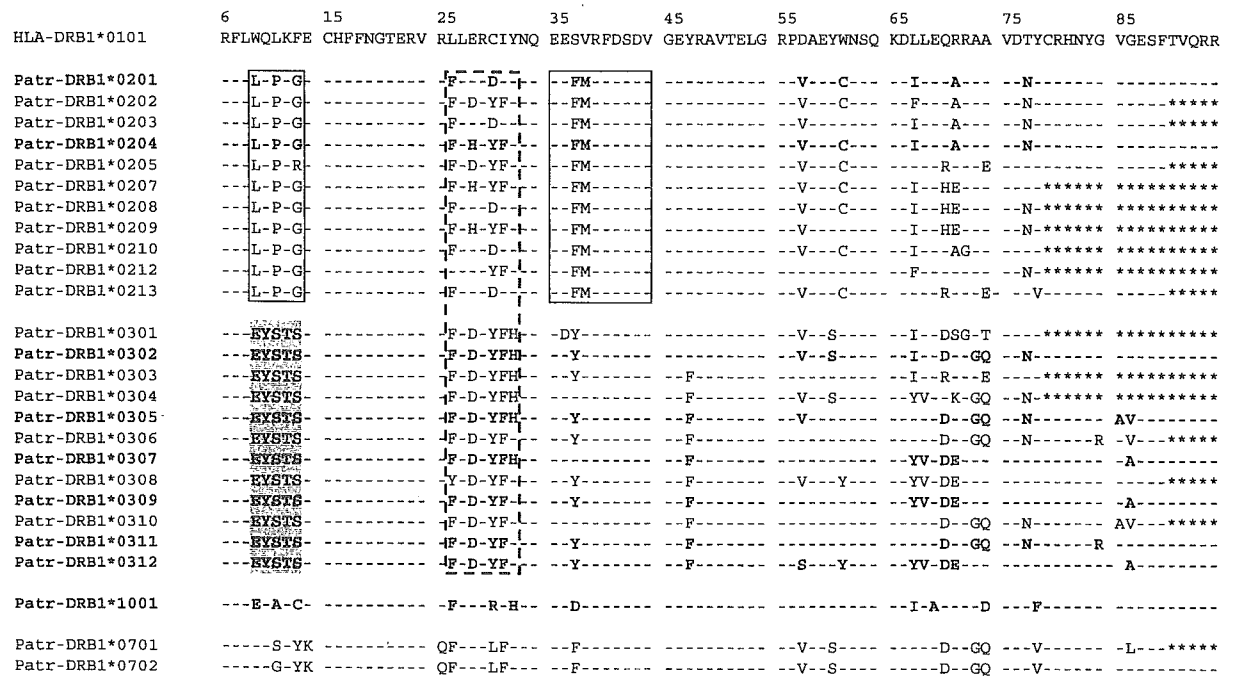

Figure 5 Alignment of the deduced amino acid sequences of Patr-DRB1 exon 2 alleles. The detected alleles in this study are highlighted by bold print. An HLA-DRB1*0101 allele is given at the top. Dashes (–) indicate identity with the consensus sequence and an asterisk (*), a lack of availability of sequence information.

and Patr-DRB1*03 lineages have converged at positions 26–32. Interestingly, the FLDRYFY motif shares some alleles of the HLA-DRB1*04 lineage. In the present study, this motif of some alleles of the Patr-DRB1*02 and Patr-DRB1*03 lineages was found to be conserved in some of the β-pleated sheet portions of the HLA-DRB1*04 lineages. These variations were thought to have been introduced by point mutations in combination with recombination within the β-pleated sheet portion in humans and chimpanzees. In addition, similar variations have been found in the β-pleated sheet portion in other primate species (26–29). Specifically, the Patr-DRB1*02 lineage shows the LQPKG amino acid motif at positions 9–13, except in the Patr-DRB1*0205 allele, and the EEFMRFDSDV amino acid motif at positions 35–44. These amino acid motifs, which appear to be of a more recent origin than the EYSTS motif of the MHC-DRB1*03 lineages, are shared in all primates and are likely to have been conserved after speciation of the Patr-DRB1*02 lineage and found only in the homnoids.

On the other hand, new alleles appear to be generated primarily by changes in the α-helical loop portion. These variations are consistent with those identified in previous studies (21, 30, 31), which suggest that the allelic variation at MHC-DRB1 has been generated primarily through exchanges in the α-helical loop portion of exon 2. Additionally, amino acid variations of Patr-DRB1 alleles at position 86 have been described in other non-human primate species (28, 32). Because the side chain of position 86 is directly related to the antigen-binding site, position 86 is known to influence DR dimer stability and the length of the peptide for the antigen-biding site (33). Therefore, these findings suggest that the differential peptide-binding function in non-human primates may be achieved by employing other types of amino acids.

In the present study, we used a 620-bp PCR technique to analyze not only the full length of exon 2 but also the sequence of a complex microsatellite located downstream of the end of exon 2. The microsatellite structure of HLA-DRB1 alleles is different among individual allelic lineages (34). However, until now, intron sequence variability of the *Patr-DRB* gene presenting among alleles within a lineage has provided only limited information. In the data provided in Table 2, the general structure of the microsatellite was strongly associated with individual lineages. Interestingly, microsatellite repeat structures such as the (GT)x(GA)y structure in Patr-DRB1*0307 differ from those in other Patr-DRB1*03 lineages. However, the microsatellite repeats of all Patr-DRB1*03 lineages have comparable lengths.

Because 620-bp PCR detected *Patr-DRB3* genes as well as *Patr-DRB1* genes, we decided to carry out a

microsatellite-PCR technique using the variable repeat length of a complex microsatellite located in intron 2 of the Patr-DRB1 and Patr-DRB3 loci. Based on the variation of microsatellite repeat patterns between Patr-DRB1 alleles and Patr-DRB3 alleles, we successfully selected Patr-DRB1 alleles.

Identification and analysis of Patr-DRB1 alleles using this method should be useful in facilitating colony management of chimpanzee groups in Japan and are expected to contribute to studies on disease association and susceptibility associated with MHC class II molecules. In addition, the data of the microsatellite sequences of the chimpanzees analyzed in the present study will provide a basis for examining the evolution of microsatellite sequences and for tracing the origin of individual Patr-DRB1 alleles.

References

1. Kenter M, Otting N, Anholts J, Jonker M, Schipper R, Bontrop RE. Mhc-DRB diversity of the chimpanzee (Pan troglodytes). *Immunogenetics* 1992: **37**: 1–11.
2. Mayer WE, O'hUigin C, Zaleska-Rutczynska Z, Klein J. Trans-species origin of Mhc-DRB polymorphism in the chimpanzee. *Immunogenetics* 1992: **37**: 12–23.
3. Brown JH, Jardetzky TS, Gorga JC et al. Three-dimensional structure of the human class II histocompatibility antigen HLA-DR1. *Nature* 1993: **364**: 33–9.
4. Walden P, Nagy ZA, Klein J. Major histocompatibility complex-restricted and unrestricted activation of helper T cell lines by liposome-bound antigens. *J Mol Cell Immunol* 1986: **2**: 191–7.
5. Louis P, Eliaou JF, Kerlan-Candon S, Pinet V, Vincent R, Clot J. Polymorphism in the regulatory region of HLA-DRB genes correlating with haplotype evolution. *Immunogenetics* 1993: **38**: 21–6.
6. Hill AV. The immunogenetics of human infectious diseases. *Annu Rev Immunol* 1998: **16**: 593–617.
7. Brok HP, Uccelli A, Kerlero De Rosbo N et al. Myelin/oligodendrocyte glycoprotein-induced autoimmune encephalomyelitis in common marmosets: the encephalitogenic T cell epitope pMOG24-36 is presented by a monomorphic MHC class II molecule. *J Immunol* 2000: **165**: 1093–101.
8. Bontrop RE. Non-human primates: essential partners in biomedical research. *Immunol Rev* 2001: **183**: 5–9.
9. Muchmore EA. Chimpanzee models for human disease and immunobiology. *Immunol Rev* 2001: **183**: 86–93.
10. Shoukry NH, Sidney J, Sette A, Walker CM. Conserved hierarchy of helper T cell responses in a chimpanzee during primary and secondary hepatitis C virus infections. *J Immunol* 2004: **172**: 483–92.
11. de Groot NG, Bontrop RE. The major histocompatibility complex class II region of the chimpanzee: towards a molecular map. *Immunogenetics* 1999: **50**: 160–7.
12. Reche PA, Reinherz EL. Sequence variability analysis of human class I and class II MHC molecules: functional and structural correlates of amino acid polymorphisms. *J Mol Biol* 2003: **331**: 623–41.
13. Bontrop RE, Otting N, de Groot NG, Doxiadis GG. Major histocompatibility complex class II polymorphisms in primates. *Immunol Rev* 1999: **167**: 339–50.
14. Elferink BG, Geluk A, Otting N et al. The biologic importance of conserved major histocompatibility complex class II motifs in primates. *Hum Immunol* 1993: **38**: 201–5.
15. Bergstrom TF, Josefsson A, Erlich HA, Gyllensten U. Recent origin of HLA-DRB1 alleles and implications for human evolution. *Nat Genet* 1998: **18**: 237–42.
16. Hughes AL. Evolution of introns and exons of class II major histocompatibility complex genes of vertebrates. *Immunogenetics* 2000: **51**: 473–86.
17. Hohjoh H, Ohashi J, Takasu M, Nishioka T, Ishida T, Tokunaga K. Recent divergence of the HLA-DRB1*04 allelic lineage from the DRB1*0701 lineage after the separation of the human and chimpanzee species. *Immunogenetics* 2003: **54**: 856–61.
18. Yoshizawa K, Ota M, Katsuyama Y et al. Genetic analysis of the HLA region of Japanese patients with type 1 autoimmune hepatitis. *J Hepatol* 2005: **42**: 578–84.
19. Hatta Y, Kanai T, Matsumoto Y, Kyuwa S, Hayasaka I, Yoshikawa Y. Analysis of cDNA coding MHC class II beta chain of the chimpanzee (Pan troglodytes). *Exp Anim* 2002: **51**: 133–42.
20. Robinson J, Waller MJ, Parham P et al. IMGT/HLA and IMGT/MHC: sequence databases for the study of the major histocompatibility complex. *Nucleic Acids Res* 2003: **31**: 311–4.
21. Bergstrom TF, Erlandsson R, Engkvist H, Josefsson A, Erlich HA, Gyllensten U. Phylogenetic history of hominoid DRB loci and alleles inferred from intron sequences. *Immunol Rev* 1999: **167**: 351–65.
22. Southwood S, Sidney J, Kondo A et al. Several common HLA-DR types share largely overlapping peptide binding repertoires. *J Immunol* 1998: **160**: 3363–73.
23. Woollard DJ, Grakoui A, Shoukry NH, Murthy KK, Campbell KJ, Walker CM. Characterization of HCV-specific Patr class II restricted CD4+ T cell responses in an acutely infected chimpanzee. *Hepatology* 2003: **38**: 1297–306.
24. Doxiadis GG, Otting N, de Groot NG, Noort R, Bontrop RE. Unprecedented polymorphism of Mhc-DRB region configurations in rhesus macaques. *J Immunol* 2000: **164**: 3193–9.
25. Otting N, de Groot NG, Noort MC, Doxiadis GG, Bontrop RE. Allelic diversity of Mhc-DRB alleles in rhesus macaques. *Tissue Antigens* 2000: **56**: 58–68.
26. Wu MS, Tani K, Sugiyama H et al. MHC (major histocompatibility complex)-DRB genes and polymorphisms in common marmoset. *J Mol Evol* 2000: **51**: 214–22.
27. Gaur LK, Nepom GT. Ancestral major histocompatibility complex DRB genes beget conserved patterns of localized polymorphisms. *Proc Natl Acad Sci USA* 1996: **93**: 5380–3.
28. Antunes SG, de Groot NG, Brok H et al. The common marmoset: a new world primate species with limited Mhc class II variability. *Proc Natl Acad Sci USA* 1998: **95**: 11745–50.
29. Nino-Vasquez JJ, Vogel D, Rodriguez R et al. Sequence and diversity of DRB genes of Aotus nancymaae, a primate model for human malaria parasites. *Immunogenetics* 2000: **51**: 219–30.

30. Erlich HA, Gyllensten UB. Shared epitopes among HLA class II alleles: gene conversion, common ancestry and balancing selection. *Immunol Today* 1991: **12**: 411–4.
31. Gyllensten UB, Sundvall M, Erlich HA. Allelic diversity is generated by intraexon sequence exchange at the DRB1 locus of primates. *Proc Natl Acad Sci USA* 1991: **88**: 3686–90.
32. Knapp LA, Cadavid LF, Eberle ME, Knechtle SJ, Bontrop RE, Watkins DI. Identification of new mamu-DRB alleles using DGGE and direct sequencing. *Immunogenetics* 1997: **45**: 171–9.
33. Demotz S, Barbey C, Corradin G, Amoroso A, Lanzavecchia A. The set of naturally processed peptides displayed by DR molecules is tuned by polymorphism of residue 86. *Eur J Immunol* 1993: **23**: 425–32.
34. Bergstrom TF, Engkvist H, Erlandsson R et al. Tracing the origin of HLA-DRB1 alleles by microsatellite polymorphism. *Am J Hum Genet* 1999: **64**: 1709–18.

doi: 10.1111/j.1744-313X.2005.00506.x

Sequence analysis of the MHC class II DPB1 gene in chimpanzees (*Pan troglodytes*)

E.-J. Bak,* Y. Ishii,* T. Omatsu,* S. Kyuwa,* I. Hayasakat & Y. Yoshikawa*

Summary

The diversity of the MHC class II region in non-human primates is a focus of biomedical research because this region plays a crucial role in the recognition of antigens in the immune system. In particular, the chimpanzee [*Pan troglodytes* (*Patr*)], which belongs to the superfamily *Hominoidea*, has been used as a human model for the study of diseases such as human hepatitis C virus (HCV), human hepatitis B virus (HBV) and human immunodeficiency virus (HIV) infections, to which only humans and chimpanzees are susceptible. In the present study, polymorphisms of the MHC-DPB1 gene (*Patr*-DPB1) in a chimpanzee colony in Japan were examined using a stepwise polymerase chain reaction (PCR) technique. In order to design a suitable primer pair which would amplify exon 2 of the *Patr*-DPB1 gene, a fragment of approximately 8 kb from exon 1 to exon 3 was amplified from chimpanzee genomic DNA. After designing a 500-bp primer pair at the 3′ region of intron 1 and the 5′ region of intron 2, analysis of DPB1 exon 2 alleles of each chimpanzee was carried out. Twenty-two chimpanzees were used in our study, and we identified seven alleles by sequence analysis on the *Patr*-DPB1 gene, including one new allele. The obtained nucleotide sequence patterns suggest that *Patr*-DPB1 alleles emerge by genetic variations such as the exchange of sequence motifs and the accumulation of point mutations.

Introduction

Major histocompatibility complex (MHC) class II molecules are highly polymorphic cell surface glycoproteins that mediate both humoral and cell-mediated immune responses. They are heterodimers comprised of two subunits which consist of an α chain and a β chain (Korman *et al.*, 1985; Slierendregt *et al.*, 1993), and the extracellular part of the α chain includes α1 and α2 domains; similarly, the β chain has β1 and β2 domains (Jones, 1997). The primate MHC class II region consists of DR, DQ and DP subregions (Slierendregt *et al.*, 1993; de Groot & Bontrop, 1999). In both humans and chimpanzees (*Pan troglodytes*), two pairs of genes are located in the DP subregion: DPA1/DPB1 and DPA2/DPB2 (Bontrop *et al.*, 1999). Although the DPA2/DPB2 genes are not functional, the DPA1 and DPB1 genes are both functional and polymorphic, leading to variation in the DP protein (Slierendregt *et al.*, 1995). Polymorphisms of MHC-DPA1/DPB1 genes are confined largely to the second exon, which encodes the functional domain that forms the peptide-binding region of the molecules (Marsh & Bodmer, 1989; Bugawan *et al.*, 1991; Klein *et al.*, 1993).

Evolutionary stability and the *trans*-species mode of inheritance have been found in many primate MHC DQ and DRB lineages (Gyllensten *et al.*, 1991; Bontrop *et al.*, 1999). Additionally, *Pan troglodytes* (*Patr*)-DPA1 alleles are closely related to some human equivalents (Otting & Bontrop, 1995; de Groot & Bontrop, 1999). However, maintenance of the DPB1 allelic variation might be controlled by a different mechanism from that of other MHC class II genes, and this mechanism may have been generated during evolutionary history. First, the primate MHC-DPB1 gene shows a relatively species-specific polymorphism, which is thought to occur by segmental recombination and point mutation within the same species. Secondly, in a survey of substitution patterns in hominoid species, the number of synonymous changes at the antigen recognition site (ARS) in hominoid DPB1 alleles was found to be only about half that for hominoid DRB1 and DQB1 alleles (Gyllensten *et al.*, 1990, 1996; Satta *et al.*, 1994), suggesting that the allelic diversification at the DPB1 loci has evolved faster than that of other MHC class loci. Lastly, in contrast to all other class II loci, the DPB1 gene appears to have been subjected to strong positive selection only in the human lineage (Hughes & Nei, 1989; Bergstrom & Gyllensten, 1995).

Because of the species-specific character of the MHC-DPB1 gene, we attempted to develop a DNA-based typing method for *Patr*-DRB1 alleles for use with the polymerase chain reaction (PCR) technique. This typing technique, in combination with direct sequencing analyses, can be effectively used to detect unique *Patr*-DPB1 alleles.

* Department of Biomedical Science, Graduate School of Agriculture and Life Sciences, The University of Tokyo, Tokyo, and † Kumamoto Primate Park, Sanwa Kagaku, Kuroiwa, Misumi-cho, Kumamoto, Japan.

Received 19 July 2004; revised 10 December 2004; accepted 22 December 2004

Correspondence: Eun-Jung Bak, Department of Biomedical Science, Graduate School of Agricultural and Life Sciences, The University of Tokyo, 1-1-1 Yayoi, Bunkyo-ku, Tokyo 113-8657, Japan.
Tel: + 81 3 5841 5038; Fax: + 81 3 5841 8186;
E-mail: missbakej@yahoo.co.jp

Materials and methods

DNA extraction

The 22 chimpanzees used in this study were housed at the Kumamoto Primate Park, Sanwa Kagaku Kenkyusho, in Japan. Table 1 lists the name, registration number, age and sex of each animal. All chimpanzees except Kirara, Kurara and Miyuki were captured in Africa and transported to Japan. The pedigree of this chimpanzee colony is available at http://www.nbr-chimp.org/chim/zoo/sanwa/sanwa-m_all.html. Miyuki and Tetsu are the parents of Kirara and Kurara. There were no other genetic relationships among the chimpanzees used in this study.

Genomic DNA was isolated from a peripheral blood sample using the QIAamp DNA Blood Mini Kit (Qiagen, Hilden, Germany) following the manufacturer's instructions.

Design of a primer set for *Patr*-DPB1 exon 2

In order to create a specific primer pair which would amplify exon 2 in each *Patr*-DPB1 allele, 8-kb PCR, covering the area from exon 1 to exon 3 on the DPB1 gene, was performed using the genomic DNA of Sanzou and Iyo (Fig. 1a and b). The primer pair (DPB-E1+ and DPB-E3–)

Table 1. Distribution of *Patr*-DPB1 alleles in individual chimpanzees

Name	Number	Age (years)	Sex	*Patr*-DPB1 alleles
Genki	53	33	Male	*13, *17
Ichigo	115	24	Female	*16, *25
Iyo	C54	27	Female	*13, *22
Izou	24	26	Male	*16, *22
Kirara[a]	277	7	Female	*13
Koiko	C51	27	Female	*11, *17
Konatu	105	27	Female	*17, *29
Kurara[a]	278	7	Female	*13
Maruku	109	24	Male	*11, *13
Miro	C30	31	Female	*13, *16
Miyuki[a]	204	19	Female	*13
Nozomi	112	26	Female	*11, *16
Remu	106	22	Female	*13
Roman	C69	30	Female	*13
Sango	C35	28	Female	*16, *22
Sanzou	C33	30	Male	*11, *13
Siomi	85	24	Female	*16
Sumiko	86	24	Female	*11, *13
Susumu	82	26	Male	*16, *17
Takabo	104	27	Male	*11, *13
Tamae	108	25	Female	*16, *17
Tetsu[a]	44	28	Male	*13, *16

[a] Miyuki and Tetue are the parents of Kirara and Kurara (identical twins).

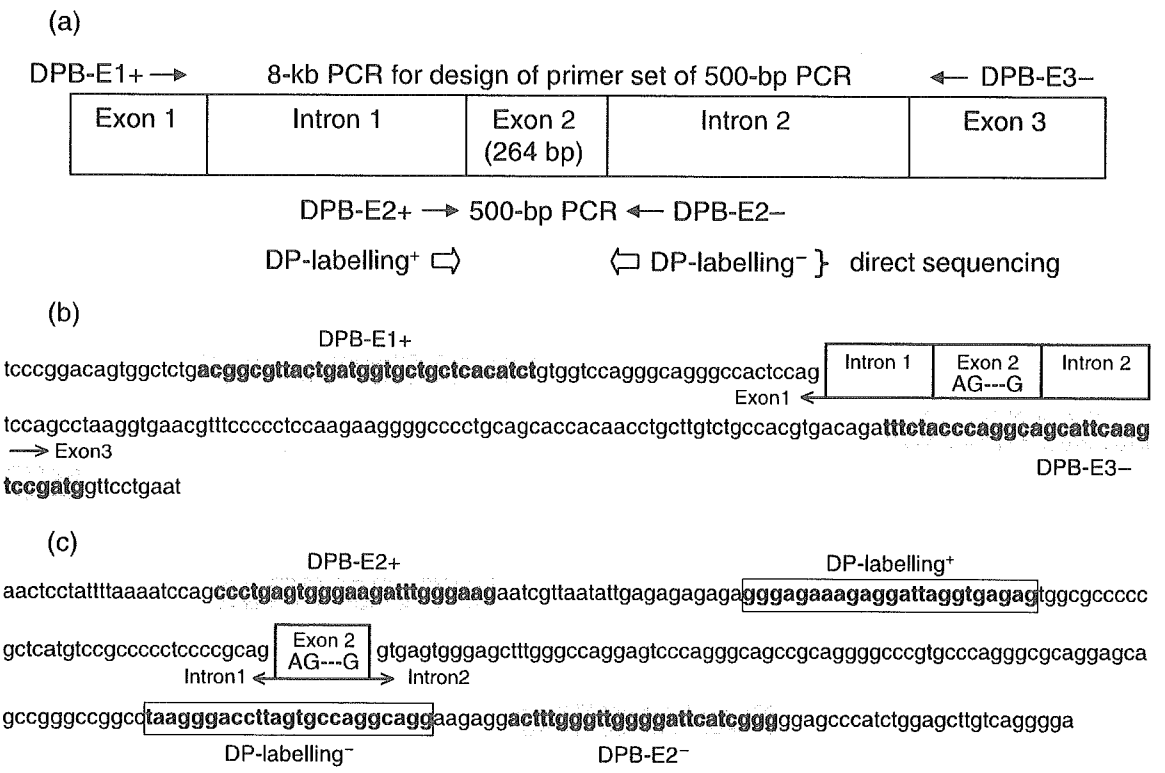

Figure 1. Designing specific primers. (a) Schematic diagram of the primer pairs used in the present study. (b) A primer pair for 8-kb PCR. DPB-E1+ and DPB-E3– (grey rectangle) are located in exon 1 and exon 3, respectively. The intron 1, exon 2 and intron 2 sequences are omitted. (c) Primer pairs for the exon 2 fragments. Grey rectangular boxes are DPB-E2+ and DPB-E2–. White boxes are DP labelling + and DP labelling – primers for direct sequences of exon 2.

was designed using a chimpanzee DP cDNA clone as previously described (Hatta *et al.*, 2002).

The reaction mixture contained 0.25 units of LA Taq polymerase (Takara, Kyoto, Japan), 2.5 mM dNTP, 2.5 mM $MgCl_2$, 4 μM of each primer, and 2 μl DNA template. Amplification was first performed with 14 cycles of denaturation at 94 °C for 20 s, and annealing and extension at 68 °C for 20 min. This was followed by 17 cycles of denaturation at 94 °C for 20 s, and annealing and extension at 68 °C for 20 min in stepwise elongation with an incubation time of 15 s/cycle. After electrophoresis in a 0.8% agarose gel (Wako, Osaka, Japan), the purified 8-kb target PCR product was ligated into a PCR-XL-TOPO vector (Invitrogen, Carlsbad, CA) and transformed into a DH5α™ competent cell (Toyobo, Osaka, Japan). The obtained clones were checked by PCR against the primer pair (sense: 5′-GCTACGCGTTTAATGGGACACAG-3′; antisense: 5′-CTCGGCGCTGCAGGGTCACGG-3′) that was used to amplify the 258-bp product of chimpanzee DPB1 exon 2. Each of four plasmid clones from Sanzou and Iyo was isolated using the NucleoSpin® Plasmid QuickPure kit (Macherey-Nagel, Düren, Germany).

The plasmid samples were then labelled with a Big Dye™ terminator v3.1 Cycle Sequencing Kit (Applied Biosystems, Foster City, CA) and analysed with an ABI PRISM™ 377 DNA Sequencer (Applied Biosystems). Based on the obtained sequences, a PCR primer pair for each chimpanzee was designed (DPB-e2+ and DPB-e2–; Fig. 1a and c) in order to amplify a 500-bp product containing the entire exon 2 (264-bp) sequences.

PCR and cloning

PCR was applied to the DNA of the 22 chimpanzees as follows. Amplification was performed using AmpliTaq Gold (Applied Biosystems) with the DPB-E2+ and DPB-E2– primers. The target products were then cloned into a pCRII-TOPO vector (Invitrogen). After transformation of the vector, 10 clones were selected for each chimpanzee.

Direct sequencing

Direct sequencing was carried out to confirm the sequence of the clones of *Patr*-DPB1 exon 2 amplified by PCR. The 500-bp products were gel-purified with a Wizard® SV gel and PCR Clean-Up System (Promega, Madison, WI) and were sequenced directly using direct sequencing primers (DP labelling + and DP labelling –; Fig. 1a and c).

MHC *Patr*-DPB1 nomenclature

The official designation for the *Patr*-DPB1 allele detected in this study was obtained from R. E. Bontrop and Natasja G. de Groot (Biomedical Primate Research Centre-TNO, Rijswijk, the Netherlands). This new allele has been registered in the DNA Data Bank of Japan (DDBJ).

Results and Discussion

Distribution of the *Patr*-DPB1 allele in each chimpanzee

Table 1 shows the patterns of *Patr*-DPB1 alleles in each chimpanzee. The *Patr*-DPB1*13 allele was found at very high frequency, being present in 13 of 22 chimpanzees. Of the five chimpanzees homozygous for DPB1*13, Kirara and Kurara are identical twins whose parents are Miyuki (*13 homozygote) and Tetsu (*13 and *16 heterozygote). A previous survey of the Biomedical Primate Research Center (BPRC) chimpanzee population showed that the *Patr*-DPB1*13, *16 and *17 alleles were the most frequently observed (Otting *et al.*, 1998). The *Patr*-DPB1*13 allele may occur frequently in the gene pool of wild chimpanzees.

Patr-DPB1 polymorphism

To date, 28 alleles of the *Patr*-DPB1 gene have been reported in the chimpanzee (Otting *et al.*, 1998; Bontrop *et al.*, 1999). In the present study, the 22 chimpanzees had seven different alleles, including one novel *Patr*-DPB1 allele. The nucleotide sequences of *Patr*-DPB1 exon 2 and the deduced amino acid sequences are depicted in Figs 2 and 3, respectively. The hypervariable region (HV) of the MHC-DPB1 exon 2 nucleotide sequence in human and non-human primate species is restricted to six major variability regions (Slierendregt *et al.*, 1995). The variations of the new allele were found in these regions, supporting the hypothesis that this new allele is not the result of random PCR error. The *Patr*-DPB1*29 allele was similar to the *Patr*-DPB1*04 allele, but was found to differ from the *Patr*-DPB1*04 allele in three non-synonymous substitutions: at codon 55 (GCT: Ala → GAT: Asp) in HV3, codon 69 (GAG: Glu → AAG: Lys) in HV4, and codon 76 in HV5 (ATG: Met → ATC: Ile) (small grey rectangular box in Fig. 2). Furthermore, the non-synonymous substitution was present at codon 24, which is located in the region immediately adjacent to the HV1-6 region (TTC: Phe → TAC: Tyr) (large grey rectangular box in Fig. 2). These variations may be considered to be point mutations.

Typing techniques for *Patr*-DPB1 alleles

Cloning and sequencing methods using PCR techniques are the traditional approach for typing MHC alleles. In MHC-DPB1 alleles which include point mutations, it is important to design a suitable primer pair for amplification of the target gene. For example, the owl monkey *Aotus nancymaae* has a unique sequence motif PLI/NRK at the C-terminus of *Aona*-DPB1 exon 2, and an attempt to amplify gene segments with a primer pair suitable for HLA-DPB1 exon 2 sequences failed (Diaz *et al.*, 2002). Also, the PCR technique using primer pairs derived from humans is limited because of the polymorphic patterns of *Patr*-DPB1 alleles. In our preliminary examination using a primer pair reported in a previously published paper (Bugawan *et al.*, 1991), three or four

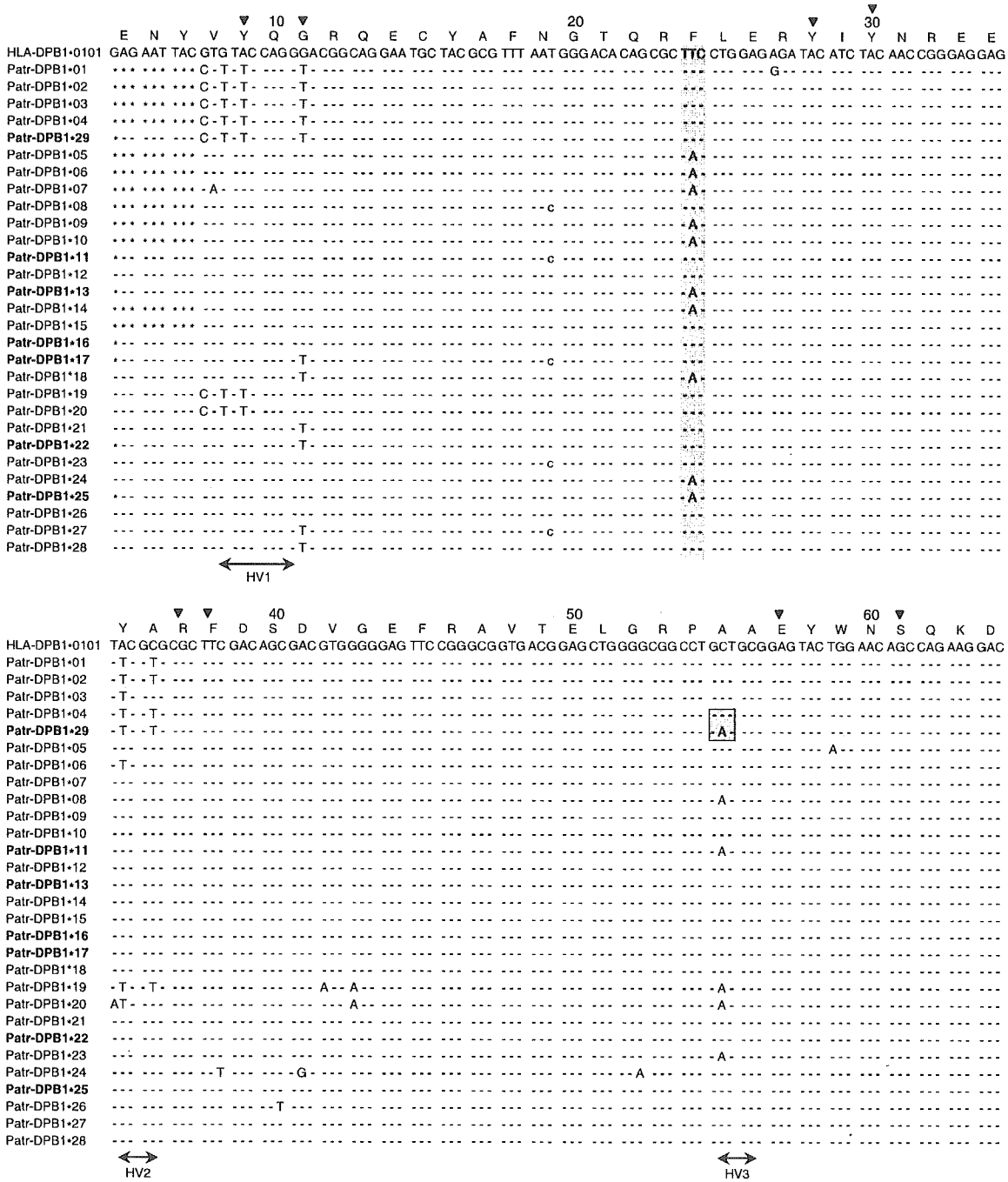

Figure 2. Alignment of the nucleotide sequences of *Patr*-DPB1 exon 2 alleles. The six previously known alleles and one new allele detected in this study are indicated by bold type (*Patr*-DPB1*29; DDBJ accession number AB183471). The HLA-DPB1*0101 allele is shown at the top of the figure. Dashes (–) indicate identity with this allele. Synonymous substitutions appear in lowercase, while non-synonymous substitutions are in uppercase. The inferred amino acid sequence of the HLA-DPB1*0101 allele is shown with the conventional one-letter code. Codons 9, 11, 28, 30, 37, 38, 57, 61, 67, 70, 71, 74, 78, 82 and 86 are antigen recognition sites (▼).

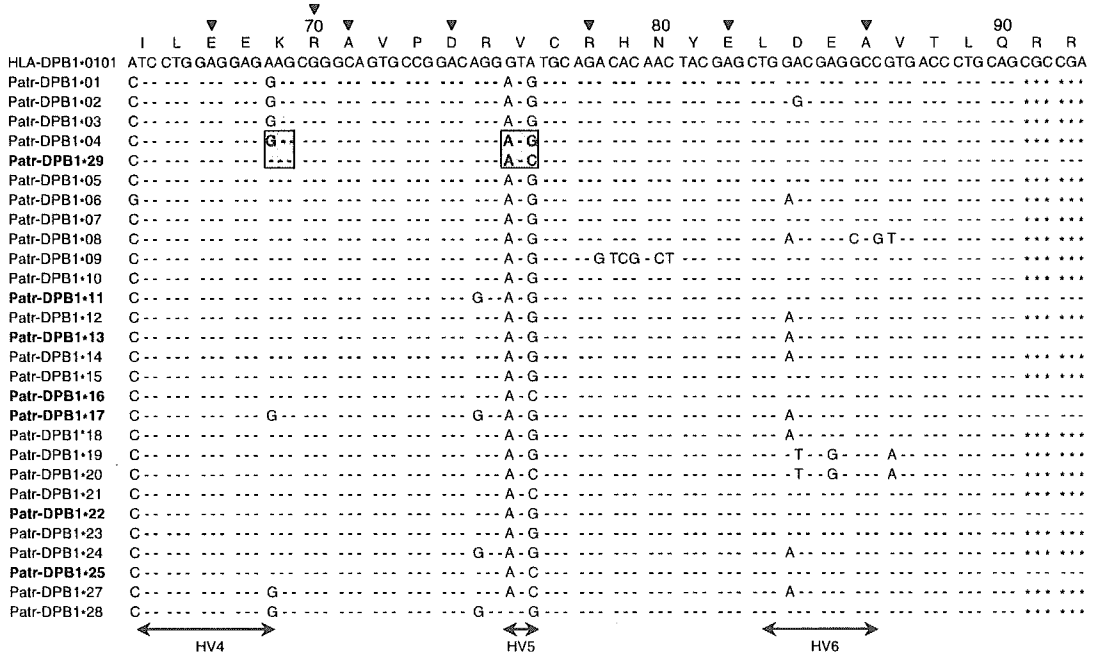

Figure 2. *Continued*

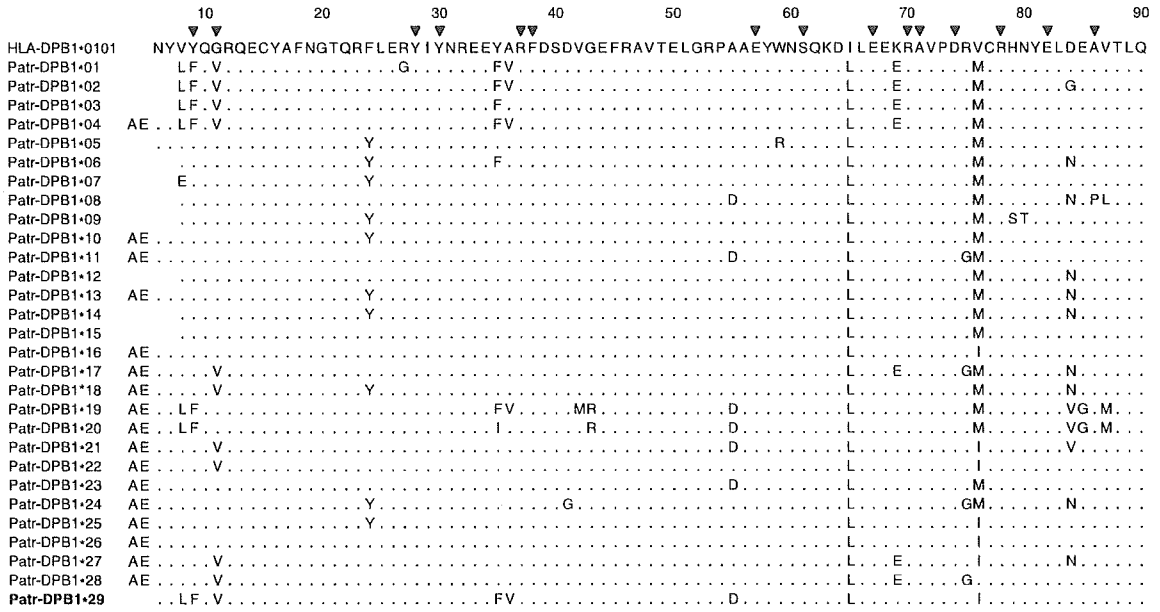

Figure 3. Alignment of the deduced amino acid sequences of 28 known *Patr*-DPB1 exon 2 alleles and one new allele detected in this study. The new allele is indicated by bold type. The HLA-DPB1*0101 allele is shown at the top of the figure. Dots (.) indicate identity with the HLA-DPB1*0101 allele. The symbol ▼ indicates antigen recognition sites.

independent alleles among selected clones were detected in some chimpanzees.

By designing a specific primer pair for the chimpanzee, we successfully analysed the exon 2 nucleotide sequences of *Patr*-DPB1 loci using cloning and direct sequencing. The application of direct sequencing was particularly useful to exclude incorrect TA cloning sequencing resulting from PCR error. The methods used in the present study should facilitate the identification of *Patr*-DPB1 alleles, and contribute towards maintenance of *Patr*-DPB1 allelic

diversity in chimpanzee groups in Japan through colony management.

References

Bergstrom, T. & Gyllensten, U. (1995) Evolution of Mhc class II polymorphism: the rise and fall of class II gene function in primates. *Immunological Review*, **143**, 13.

Bontrop, R.E., Otting, N., de Groot, N.G. & Doxiadis, G.G. (1999) Major histocompatibility complex class II polymorphisms in primates. *Immunological Review*, **167**, 339.

Bugawan, T.L., Begovich, A.B. & Erlich, H.A. (1991) Rapid HLA-DPB typing using enzymatically amplified DNA and nonradioactive sequence-specific oligonucleotide probes. *Immunogenetics*, **34**, 413.

Diaz, D., Daubenberger, C.A., Zalac, T., Rodriguez, R. & Patarroyo, M.E. (2002) Sequence and expression of MHC-DPB1 molecules of the New World monkey *Aotus nancymaae*, a primate model for *Plasmodium falciparum*. *Immunogenetics*, **54**, 251.

de Groot, N.G. & Bontrop, R.E. (1999) The major histocompatibility complex class II region of the chimpanzee: towards a molecular map. *Immunogenetics*, **50**, 160.

Gyllensten, U.B., Lashkari, D. & Erlich, H.A. (1990) Allelic diversification at the class II DQB locus of the mammalian major histocompatibility complex. *Proceedings of the National Academy of Sciences of the USA*, **87**, 1835.

Gyllensten, U.B., Sundvall, M. & Erlich, H.A. (1991) Allelic diversity is generated by intraexon sequence exchange at the DRB1 locus of primates. *Proceedings of the National Academy of Sciences of the USA*, **88**, 3686.

Gyllensten, U., Bergstrom, T., Josefsson, A., Sundvall, M. & Erlich, H.A. (1996) Rapid allelic diversification and intensified selection at antigen recognition sites of the Mhc class II DPB1 locus during hominoid evolution. *Tissue Antigens*, **47**, 212.

Hatta, Y., Kanai, T., Matsumoto, Y., Kyuwa, S., Hayasaka, I. & Yoshikawa, Y. (2002) Analysis of cDNA coding MHC class II beta chain of the chimpanzee (*Pan troglodytes*). *Experimentation Animale*, **51**, 133.

Hughes, A.L. & Nei, M. (1989) Nucleotide substitution at major histocompatibility complex class II loci: evidence for overdominant selection. *Proceedings of the National Academy of Sciences of the USA*, **86**, 958.

Jones, E.Y. (1997) MHC class I and class II structures. *Current Opinions in Immunology*, **9**, 75.

Klein, J., Satta, Y., O'hUign, C. & Takahata, N. (1993) The molecular descent of the major histocompatibility complex. *Annual Review of Immunology*, **11**, 269.

Korman, A.J., Boss, J.M., Spies, T., Sorrentino, R., Okada, K. & Strominger, J.L. (1985) Genetic complexity and expression of human class II histocompatibility antigens. *Immunological Review*, **85**, 45.

Marsh, S.G. & Bodmer, J.G. (1989) HLA-DR and -DQ epitopes and monoclonal antibody specificity. *Immunology Today*, **10**, 305.

Otting, N. & Bontrop, R.E. (1995) Evolution of the major histocompatibility complex DPA1 locus in primates. *Human Immunology*, **42**, 184.

Otting, N., Doxiadis, G.G., Versluis, L., de Groot, N.G., Anholts, J., Verduin, W., Rozemuller, E., Claas, F., Tilanus, M.G. & Bontrop, R.E. (1998) Characterization and distribution of Mhc-DPB1 alleles in chimpanzee and rhesus macaque populations. *Human Immunology*, **59**, 656.

Satta, Y., O'hUign, C., Takahata, N. & Klein, J. (1994) Intensity of natural selection at the major histocompatibility complex loci. *Proceedings of the National Academy of Sciences of the USA*, **91**, 7184.

Slierendregt, B.L., Kenter, M., Otting, N., Anholts, J., Jonker, M. & Bontrop, R.E. (1993) Major histocompatibility complex class II haplotypes in a breeding colony of chimpanzees (*Pan troglodytes*). *Tissue Antigens*, **42**, 55.

Slierendregt, B.L., Otting, N., Kenter, M. & Bontrop, R.E. (1995) Allelic diversity at the Mhc-DP locus in rhesus macaques (*Macaca mulatta*). *Immunogenetics*, **41**, 29.

霊長類を用いた脳梗塞モデルの遺伝子治療研究

東京大学大学院農学生命科学研究科　獣医学専攻実験動物分野　教授　吉川　泰弘

我々の研究班では「霊長類、サルを用いた脳梗塞モデルの作成とそのモデルを用いた遺伝子治療の研究」を進めております。その内容について簡単に説明したいと思います。

研究の背景について最初に述べます。わが国では、少子高齢化が猛烈な勢いで進んでいるわけで、2030年頃までの予測では65歳以上の高齢者が少なくとも全人口の30%以上を占める、超高齢社会を迎えるというふうにいわれています。予測といっても人の寿命は長いですからほとんど外れようのないシミュレーションだと思います。先進国の中で、いろいろな国々を見ても、ロングタームで高齢化してきた社会はヨーロッパにもいくつかありますけれども、こんな急速な、私も団塊の世代の一人なんですけれども、高齢化が進む国はなかなかありません。そのためたぶんモデルを捜すというよりは、自分たちで問題を解決していくという姿勢が必要であろうと思います。

特にそうした中で老人病というのは大きな問題になるわけです。われわれが取り組もうとしている血管性痴呆というのは、患者数の多さ、いったんなったあとの高齢者のQOLの低下、孤立、あるいは社会的な負担の大きさというものを考えると、非常に大きなテーマであろうと思います。われわれの研究班ではサル類を用いて脳梗塞のモデルを作成しよう、そして、そのモデルを使って遺伝子治療による後遺症の軽減を図ることを目的としています。

この研究を申請したときに、「従来の遺伝子治療という概念からすると、脳梗塞に遺伝子治療という組み合わせはちょっとめずらしい」という指摘をいただきました。確かに初期の遺伝子治療というのは、25年前に米国で、10年前に北大で行われたADA（アデノシン・ディアミナーゼ欠損症）を含めて遺伝病の治療という考えが多かったのですけれども、その後、使い方に関してはいろいろな多様性を持ってきました。特に脳梗塞の後に起こる神経細胞のアポトーシスというものは、時間軸上急速に進むわけで、そこを何とかうまく乗り切れれば後遺症を軽減できるのではないかというわけです。そういう意味からすれば、常時連続的な遺伝子発現でなくても急速な高用量の発現でアポトーシスをブロックできればいけるのではないかというのがわれわれの基本的な考え方です。それに合うベクターは何かというところから始まるわけです。これは、ヒトの左の中大脳動脈の閉塞で、ここのところで閉塞が起こった像です（図１）。

研究班の特性を最初に述べたいと思いますけれども、目的は先ほど言いましたように、脳梗塞に伴う神経細胞死、これを軽減する安全有効な遺伝子治療法を確立しようということです。

モデルとしては、ヒトにもっとも近縁なサル類を用いた脳梗塞、脳虚血のモデルをまず作るということ、そのモデルを用いて、センダイウイルスベクターを用いた治療法を検討するということ、また治療の評価ということになるわけですけれども、サル類ですから、マウスやラットとは違った脳機能の評価法というものがあります。そういった新しい評価法に基づく治療の有効性、安全性の確認をしようという目的で進んでおります。

特徴としては、齧歯類のモデルでやってきたものを今回サルにあげるわけで、臨床応用可能なサル類での疾患モデルを作成する。すなわち、齧歯類モデルのテクノロジーを使ってヒトへのトランスレーショナルリサーチ・モデルとしてサルで脳虚血、あるいは大血管、微小血管脳梗塞モデルを作成する。そして、多くの遺伝子治療は、もともとアメリカで始まって、アデノウイルスを含めてAAVもレトロウイルスもほとんど国産のベクターというのを使う機会はなかったのですけれども、先ほど言ったような、短期間の高用量発現に適したベクターがいいというアプローチをしてきましたので、わが国独自に開発されたセンダイウイルスベクターを用いようということでやっております。

また、虚血性脳血管障害の臨床応用に可能なプロトコールを作成しようということで、多彩な共同研究になっております。医師、獣医師、基礎科学者ということで、東大は医学部の脳神経外科、私は農学部の獣医ですけれども、元の理学部の新領域創生科学、元々自分がいた厚生省の筑波霊長類センター、ベクター開発のデイナベック、九州大学医学部といったグループで進めております（図２）。

最初にこれまでの成果を簡単にレビューしていきたいと思います。

一つは、ベクターとなるセンダイウイルスの改良です。センダイウイルスには、いい面も悪い面もありますけれども、センダイウイルスベクターというのは、とにかく日本で独自に開発されたベクターである。日の丸ベクターと言われたときもありました。センダイウイルスはRNAのシングルストランドのネガティブウイルスです。最大3,5キロベースの外来遺伝子を乗っけることが可能です。ウイルスが細胞に侵入する際のレセプターはシアル酸ですから、細胞のどこでも発現していて、どの細胞でも感染可能です。細胞融合活性が非常に強くて、昔、遺伝子を細胞内に入れるときにセンダイウイルスを融合するための道具として使ったわけですけれども、導入した遺伝子を早期に非常に高く発現します。これはアデノウイルスとか他のウイルスの100倍とか1000倍というオーダーです。ただ、ゲノムに乗るわけではないので、一過性の発現、それも核内にはいかないんで、細胞質内での発現ということになります。

逆に言えば染色体に組み込まれるわけではないので、レトロウイルスとは違いまして、非分裂の細胞でも平気で感染しますし、細胞質内で増殖するので、染色体に影響するということはありません。ただ、そういう意味で発現を持続させるという点が難しい。

もう一つの欠点が、細胞障害性が強いという点です。ベクターは今第３世代まできています。最初は野生型の付加型でした。これはセンダイウイルスのゲノム構造が、NP-P-M-F-HN-Lという格好で上流から並んでいますけれども、いちばん上流に外来遺伝子を入れます。メッセンジャーのでき方は、上流から順に読み取り効率が悪くなるという特徴がありますので、いちばん上流にいれます。

野生型は非常に増殖性がいいんですけれども、感染性粒子が産生され当然2次感染を起こしますし、細胞障害性が非常に強い。細胞を障害する非常に大きな因子は先ほど言いました融合蛋白、F蛋白です。そのため第1世代としては、F蛋白欠損のウイルスを作るということになりました。こうすると、非感染粒子は放出します。M蛋白遺伝子がありますから粒子は形成されます。マトリックス蛋白を作って粒子はできるけれども、直接の細胞障害性というのは、少し軽減されます。第2世代のFM欠損ウイルス、これをしますと、ウイルス粒子そのものが形成されないという形になって、より細胞障害性は低くなります。それでもHNがありますから、抗原性などの影響がまだ残るということで、3世代目のは、MFHトリプルの欠損型というものを作っております（図3）。

サル類の実験に入るにあたって、ベクターの有効性と安全性が最初の問題になります。実はこの研究を始めたときには、センダイウイルスは元々齧歯類のウイルスですから、霊長類に対してどういうふうに振舞うかという情報がなくて、一番最初の実験は、P3の中で、筑波霊長類センターでやりました。問題の一つは本当に増えるかどうかということで、カニクイザルの初代培養細胞で、このベクターが増えるであろうか？増えてもいいのですけれども、水平感染を起こしてどんどん広がっていくようですと、これはまた治療ベクターとして問題なので、水平感染が起こるか起こらないかということを調べたわけです。実際には、一歳齢のカニクイザルを用いて、片方にセンダイウイルスを1×10^9接種して、もう一頭は同居個体として水平感染を調べるということを繰り返したわけですけれども、接種個体は抗体がすぐにあがっていきますが、同居個体には抗体上昇がないということで、かなり密な接触ですから、水平感染は起こらないという結論を得て、その後の実験はP2で行えるようになっております。現在はP2でやっています。

もう一つはカニクイサルの胎児、80日から90日齢で胎児からいろいろな初代培養細胞を作成して神経、肺、腎臓、その他、消化管、あるいは結合組織といったような細胞を採って、センダイウイルスをかけますと、どの細胞でも非常によく増えます。欠点は4日目くらいからCPEが出てしまうという点であります。いろいろな細胞を試してみると、神経系と肺は非常に増殖が安定していていいということがわかりました。意外だったのはリンパ系での増殖はけっしてよくない。骨髄細胞では多少増えますけれども、分化したリンパ球ではセンダイウイルスはサルの場合、増殖が悪いという結論であります。それからin vivoにおける有効性と安全性ということで、センダイウイルスを接種して、どういう病変が惹起されるか確かめました。有効性試験は九大ですでに臨床研究に入りましたけれども、ヒトに使う前臨床試験として、この場合は筋肉内投与で評価をしたわけです。ヒトの常用量と10倍量の高用量の両方を接種して有効性と安全性を見た試験です。安全性試験では左右前頭葉、眼球、鼻腔内、肝臓、脾臓、腎臓、いろいろな場所にウイルスを接種して調べたわけですけれども、接種の5日から10日の間に、急性の毒性反応というものはありませんでした。しかし、顕微鏡レベルでは、肉眼的には特に病変はないのですけれども、病理組織学的には、接種した臓器に炎症反応があって、これは脳の病変ですけれども、囲管性細胞浸潤が接種部位に隣接して見られます。

特に問題点として、非欠損のワイルドタイプのベクターを打ちますと、脳室内接種では